Mechanical Anisotropy of Rat Aortic Smooth Muscle Cells Decreases with Their Contraction*
(Possible Effect of Actin Filament Orientation)

Kazuaki NAGAYAMA** and Takeo MATSUMOTO**

Tensile properties of smooth muscle cells freshly isolated from rat thoracic aortas (FSMCs) in their major and minor axes were measured using a laboratory-made micro tensile tester. The relationship between the tension applied to a cell and its elongation was obtained in untreated cells and those treated with 10^{-5} M serotonin to induce contraction. An initial stiffness of untreated FSMCs, normalized by their initial cross-sectional area perpendicular to the stretch direction, was significantly higher in the major axis (14.8 ± 4.3 kPa, mean ± SEM, $n = 5$) than the minor axis (2.8 ± 1.0 kPa, $n = 5$). The stiffness increased significantly in response to the contraction, but the increase was much higher in the minor axis (59.0 ± 9.4 kPa, $n = 4$) than in the major (88.1 ± 13.3 kPa, $n = 4$). The difference between the two directions was insignificant in the contracted state. Observations of the morphology of actin filaments with a confocal laser scanning microscope in untreated FSMCs revealed that they were long fibers running almost parallel to the major axis, while those in contracted cells showed an aggregated structure without a preferential direction. These results may indicate that anisotropy in untreated FSMCs is caused by the anisotropic alignment of their actin filaments, and that such anisotropy disappears in response to actin filament reorganization caused by the contraction.

Key Words: Cellular Biomechanics, Mechanical Properties, Smooth Muscle Contraction, Normalized Stiffness, Stress Fibers

1. Introduction

Smooth muscle cells (SMCs), one of the main components of arterial walls, contract and relax in response to mechanical and chemical stimuli, which leads to corresponding changes in blood vessel diameter. The mechanical properties and dimensions of SMCs change in response to variation in the in vivo mechanical environment to which they are exposed[1]–[3]. To study the mechanical environment in the arterial wall in detail under various physiological conditions, it is important to know the mechanical properties of SMCs in the contracted and relaxed states. Aortic smooth muscle cells are spindle-shaped and aligned almost parallel to the circumferential direction of the arterial wall. Their intracellular contractile apparatus, such as actin filaments and myosin filaments, run mostly parallel to their major axis, and their contraction takes place in that direction. Actin filaments have a close correlation with the mechanical properties of cells[4]–[6]. Thus, the mechanical properties of SMCs may be anisotropic. To our knowledge, however, there have been no reports on the anisotropic mechanical properties of SMCs.

SMCs change their dimensions and mechanical properties drastically in response to their contraction. It has been reported that SMCs isolated from the rat thoracic aorta with enzymatic digestion shortened by 30% in response to norepinephrine[7]. Matsumoto et al.[8] reported that rat aortic SMCs displayed a 10-fold increase in their elastic modulus in response to their contraction. Such large changes should have considerable effects on their internal force balance and actin filament orientation. Thus, the mechanical anisotropy of SMCs may change in response to their contraction.

In this study, we measured tensile properties of freshly isolated SMCs (FSMCs) in their major and minor axis directions using a cell tensile tester developed in our laboratory[9]. We also used FSMCs treated with 10^{-5} M serotonin to induce their contraction, measured the tensile properties of the contracted cells in their major and

* Received 7th June, 2004 (No. 04-4148)

** Biomechanics Laboratory, Department of Mechanical Engineering, Nagoya Institute of Technology, Gokiso-cho, Showa-ku, Nagoya 466–8555, Japan.
E-mail: k-nagaym@nitech.ac.jp

minor axis directions, and examined the effect of cell contraction on the anisotropy of cells. We also observed the morphology of actin filaments in both untreated and contracted FSMCs with a confocal laser scanning microscope to investigate the effect of actin filament morphology on the mechanical anisotropy of FSMCs.

2. Materials and Methods

2.1 Preparation of freshly isolated smooth muscle cells (untreated FSMCs)

All animal experiments and treatments were conducted in accordance with the *Guide for Animal Experimentation*, *Nagoya Institute of Technology*. Male Wistar rats (8 – 14 weeks of age) were killed by suffocation in a CO_2 chamber before their thoracic aortas were quickly excised. FSMCs were isolated from aortic tissue by enzymatic digestion, which is a slight modification of Chamley et al.[10] Briefly, the excised aortas were placed in a phosphate buffered saline (PBS, Nissui) and loose connective tissues were removed from their surface. The aortas were then cut into tubular segments, whose lengths were about 10 mm, and stored at 4°C for 1 – 4 h. Each segment was then placed in a 2 mL Ca^{2+}-Mg^{2+}-free Hank's balanced salt solution (HBSS(-), Sigma) at 37°C containing 300 U of collagenase type III (Worthington Biochemical) and 1.8 U of elastase type I (Sigma), and gently shaken at a rate of 50 cycle/min for 1.5 h. The adventitia of the aortic tissue was separated by pipetting and removed using a pair of forceps. The remaining tissue was placed into 2 mL of the fresh enzyme solution and shaken again for 0.5 – 1 h to yield an FSMC suspension. The cell suspension was filtered by a cell strainer (40 μm Nylon, Falcon) to remove excess tissue, and diluted in HBSS(-) to about 1 : 10 to reduce the effect of the enzymes. Cells were used for the tensile test within three hours of the dilution, and were stored at 4°C until they were used. Untreated FSCMs possessing an axial length of more than 20 μm and a smooth-looking surface (Fig. 1 (a)) were used for the tensile test.

2.2 Preparation of contracted smooth muscle cells (contracted FSMCs)

The cells obtained in the previous section were used as the source of contracted FSMCs. The FSMCs were treated with HBSS(-) containing 10^{-5} M Ca^{2+} and 10^{-5} M serotonin (5-hydroxytryptamine, Sigma) at 37°C. The cell image was obtained with a cooled digital CCD camera (ORCA-ER, Hamamatsu Photonics) and recorded in a personal computer to confirm their contraction. Cell shortening in the major axis direction ε_s was measured with image analysis software (MetaMorph Ver6.0, Universal Imaging). We used cells that finished their morphological changes (cell shortening and membrane bleb formation) (Fig. 1 (b)) within 20 min of treatment with the agonists.

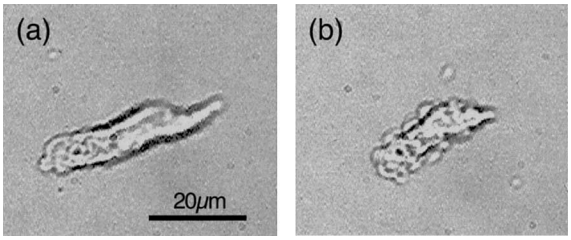

Fig. 1 Phase contrast images of a freshly isolated rat aortic smooth muscle cell before (a) and after (b) treatment with serotonin (10^{-5} M).

2.3 Cell tensile tester

The cell tensile tester used for the present study was a modification of that reported previously[9], which consisted of an upright microscope, a computer-controlled electric micromanipulator (MMS-77, Shimadzu), a manual micromanipulator (MHW-3, Narishige), and an analog CCD camera (TM1650B, Toshiba). In this study, we used an inverted microscope (TE2000E, Nikon) and the cooled digital CCD camera instead of an upright microscope and an analog CCD camera. An arm made from a glass micropipette, whose tip diameter was about 10 μm, was set on each micromanipulator. A cell in the dish was held with two glass micropipettes: an operation pipette and a deflection pipette. Originally, the cell was held by aspirating into the two micropipettes. In this study, the cell was held by gently pressing onto its surface two pipettes that had been coated with a urethane resin adhesive (Sista M5250, Henkel)[11),(12)]. We have already confirmed that the tensile properties obtained from SMCs using the two methodologies were almost similar[13]. An operation pipette was moved with the electric micromanipulator to stretch the cell horizontally. The tension applied to the cell was measured by the deflection of the cantilever part of the deflection pipette. After tensile testing, the spring constant of the deflection pipette was determined through calibration with a reference pipette. In this study, the spring constant of deflection pipettes was within the range 0.016 – 0.353 N/m.

2.4 Tensile test

We set a cell culture dish containing the cells suspended in HBSS(-) on the microscope stage, whose temperature was controlled at 37°C, and waited for about 10 min until the temperature of the suspension reached the preset value. A cell in the dish which met the criteria described in sections 2.1 and 2.2 was randomly selected and held with the two micropipettes coated with the adhesive. When the cell was stretched along its major axis, each of the glass micropipettes was gently pressed down on each end of the cell (Fig. 2 (a)). The cell was held gently on both sides with the two pipettes (Fig. 2 (b)) when stretched in the minor axis direction. After waiting for about 5 minutes to make the adhesion between the cell and the pipettes firm, we stretched the cell stepwise by moving the operation pipette 1 μm every 5 seconds until fracture occurred, or until the cell began to slip off from

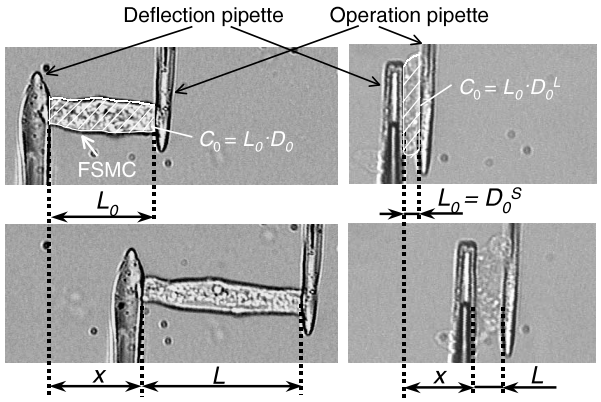

(a) Stretch in major axis direction (b) Stretch in minor axis direction

Fig. 2 Smooth muscle cells stretched in their major (a) and minor (b) axis directions during the tensile test.

the pipette. The cell image was recorded during the stretch procedure via a CCD camera connected to a personal computer. Specimens were not preconditioned to eliminate possible stretch-induced contraction of the cells.

2.5 Evaluation of mechanical properties of the cells

After the tensile test, the recorded images were analyzed with the image analysis software. We measured the distance between the two pipettes, L, and the displacement of the deflection pipette, x. The tension applied to the cell T was calculated by multiplying x with the spring constant of the deflection pipette, k, which was measured after each experiment. The elongation of the cell ΔL was calculated as the increment of L. To reduce the effect of cell dimension on mechanical properties, we normalized the tension T with the initial cross-sectional area of the cell A_0, as given by $\sigma = T/A_0$, and refer to it as normalized tension. When we estimated A_0 for a cell stretched along its major axis, we calculated the initial diameter of the cell D_0 by dividing the initial tracing area of the cell C_0 with the initial distance between the two pipettes L_0, as given by $D_0 = C_0/L_0$, and assumed that the cell cross-sectional shape perpendicular to the stretch direction was circular, such that $A_0 = \pi(D_0/2)^2$ (Fig. 2 (a)). We assumed that the cell cross-sectional shape perpendicular to the stretch direction in a cell stretched along the direction of its minor axis was an ellipse with major and minor diameters D_0^L and D_0^S, respectively. The initial major diameter D_0^L was calculated as D_0, as mentioned above, such that $D_0^L = C_0/L_0$. The initial minor diameter D_0^S was assumed to be equal to the initial distance between the two pipettes L_0 (Fig. 2 (b)). The nominal strain ε was obtained by normalizing the elongation ΔL with the initial distance of the two pipettes, L_0.

Mechanical properties of the cells were evaluated with tension – elongation ($T - \Delta L$) and normalized tension – nominal strain ($\sigma - \varepsilon$) curves. The initial stiffness S_{ini} was obtained by fitting a straight line from the origin to the region where the elongation was smaller than 3 μm in $T - \Delta L$ curves. The initial normalized stiffness E_{ini} was obtained by fitting a straight line from the origin to the low strain region ($\varepsilon < 0.2$) of $\sigma - \varepsilon$ curves.

2.6 Observation of actin filament morphology in FSMCs

We observed actin filament morphology in both untreated and contracted FSMCs by fluorescent staining. The cells in the culture dish were fixed with PBS containing 3.7% formaldehyde for 5 min, and rinsed gently with plain PBS. The cells were then treated with PBS containing 0.1% Triton X-100 (ICN Biomedicals) for 5 min, and stained with rhodamine-phalloidin (Molecular Probes) in PBS for 20 min at room temperature. These operations were performed very carefully to avoid the movement of cells beyond the view from the microscope. Actin filaments stained with rhodamine-phalloidin were observed using an inverted microscope combined with a confocal laser scanning system (DIGITAL ECLIPSE C1, Nikon). Optically sectioned images (0.35 – 0.80 μm steps) were collected and reconstructed to form a plane image.

2.7 Statistical analysis

Data are expressed as mean ± SEM. Differences were analyzed by the Student's paired and unpaired t-test, and were considered significant when $P < 0.05$.

3. Results

Figure 1 shows an example of FSMCs before and after contraction induced with HBSS(-) containing 10^{-5} M Ca^{2+} and 10^{-5} M serotonin. About 20% of the cells responded to the agonists, and their contractions finished within 20 min after treatment. The surface of FSMCs looked smooth before the induction of the contraction (Fig. 1 (a)), but some of the contracted FSMCs had blebs on their surface (Fig. 1 (b)). The length of untreated FSMCs was 38.8±2.4 μm ($n = 17$) and 9.5±0.5 μm ($n = 17$) along their major and minor axis, respectively. In contracted FSMCs, the length of the cells was 24.4 ± 1.3 μm ($n = 8$) and 9.6 ± 0.6 μm ($n = 8$) along their major and minor axis, respectively. The difference in cell size between the two types of cells was significant for the major axis length, but not the minor. Cell shortening along the major axis direction ε_s was 29.1 ± 3.1% ($n = 8$).

Tension – elongation curves in major and minor axis directions were obtained for the two groups (Fig. 3). There was no significant difference in the initial slopes of the untreated cells between the major and minor axis directions: initial stiffness S_{ini} of the untreated cell was 0.070±0.016 N/m ($n = 5$) and 0.097±0.025 N/m ($n = 5$) for the major and minor directions, respectively. The slope of the curves of the contracted cells was remarkably steeper than that of untreated cells. The initial stiffness of the contracted cell was significantly higher ($P < 0.05$) in the mi-

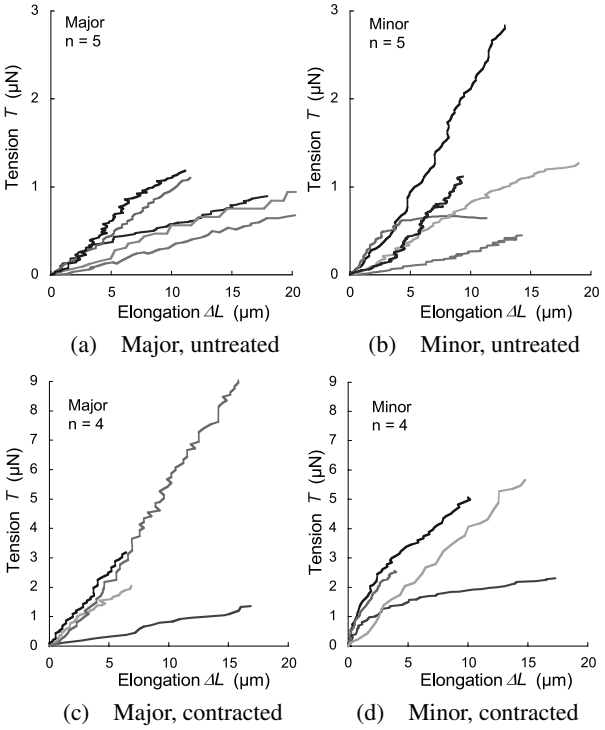

(a) Major, untreated (b) Minor, untreated

(c) Major, contracted (d) Minor, contracted

Fig. 3 Tension – elongation curves of the FSMCs. The untreated cells stretched in their major (a) and minor (b) axis directions, and the contracted cells stretched in their major (c) and minor (d) axis directions.

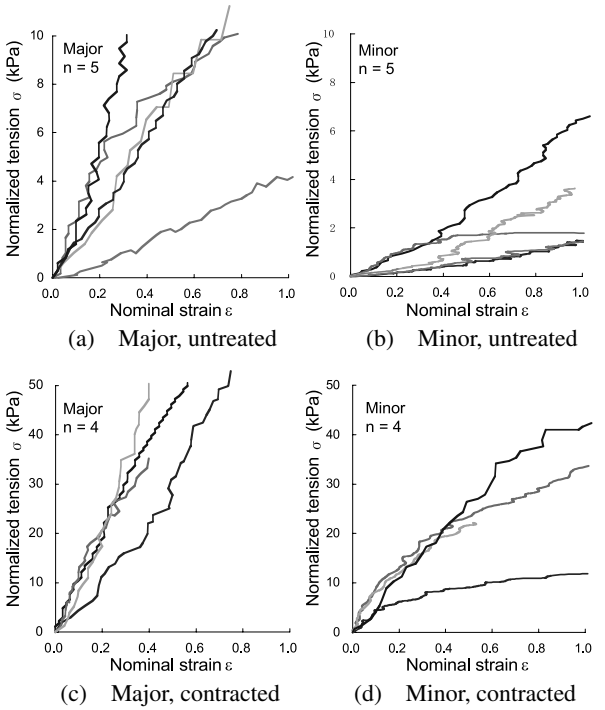

(a) Major, untreated (b) Minor, untreated

(c) Major, contracted (d) Minor, contracted

Fig. 4 Normalized tension – nominal strain curves of the FSMCs. The untreated cells stretched in their major (a) and minor (b) axis directions, and the contracted cells stretched in their major (c) and minor (d) axis directions.

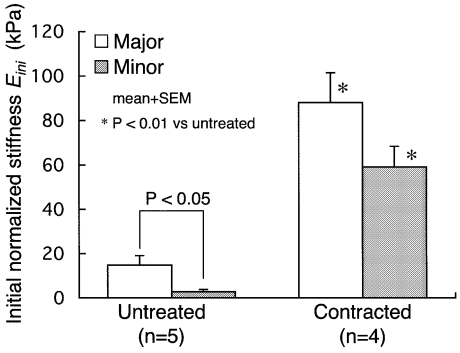

Fig. 5 Summary of the initial normalized stiffness of FSMCs.

nor direction (0.595 ± 0.117 N/m, $n = 4$) than in the major (0.187 ± 0.046 N/m, $n = 4$).

The normalized tension – nominal strain curves in major and minor axes are shown in Fig. 4. The relationship between the normalized tension and nominal strain was relatively linear in the major and minor axis directions in untreated FSMCs, and in the major axis in contracted FSMCs. In contrast, the curve of contracted FSMCs in the minor axis direction showed marked curvilinearity. In untreated FSMCs, the slopes in the major axis looked steeper than those in the minor axis (Fig. 4 (a) and (b)). On the other hand, the slope of the curves in contracted FSMCs seems to show little difference between major and minor axis directions (Fig. 4 (c) and (d)). The tensile properties of the two groups stretched in the two directions are compared quantitatively in Fig. 5. E_{ini} of untreated FSMCs was significantly higher in the major axis (14.8 ± 4.3 kPa, $n = 5$) than in the minor axis (2.8 ± 1.0 kPa, $n = 5$), indicating that freshly isolated SMCs are anisotropic. In contracted FSMCs, E_{ini} was significantly higher than that obtained for untreated FSMCs in both directions, but the difference between the two directions was insignificant in contracted FSMCs: E_{ini} was 88.1 ± 13.3 kPa ($n = 4$) and 59.0 ± 9.4 kPa ($n = 4$) for the major and minor axis, respectively.

The relationship between the initial normalized stiffness E_{ini} in contracted FSMCs and cell shortening ε_s along the direction of the major axis is shown in Fig. 6. Cell shortening shows a significant positive correlation with E_{ini} in the major axis direction, but not with E_{ini} in the minor axis direction.

Actin filaments in untreated FSMCs were observed as long and thick fibers running almost parallel to the direction of the major axis (Fig. 7 (a) and (b)). The actin filaments in contracted cells looked entangled and possessed bulk-like structures, and appeared to exhibit no preferential direction (Fig. 7 (c) and (d)).

4. Discussion

We investigated the mechanical anisotropy of freshly isolated smooth muscle cells obtained from rat thoracic aortas, and found that (a) freshly isolated smooth muscle

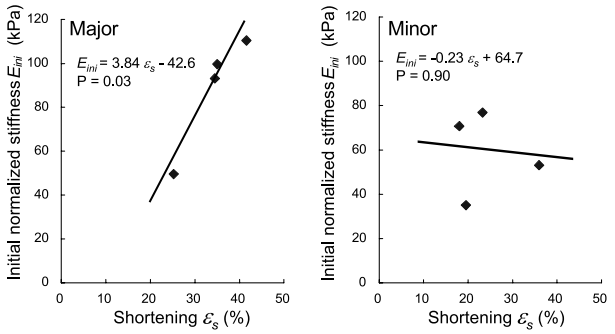

(a) Stretch in major axis direction (b) Stretch in minor axis direction

Fig. 6 Relationships between the initial normalized stiffnesses E_{ini} of the contracted FSMCs and their shortening ε_s.

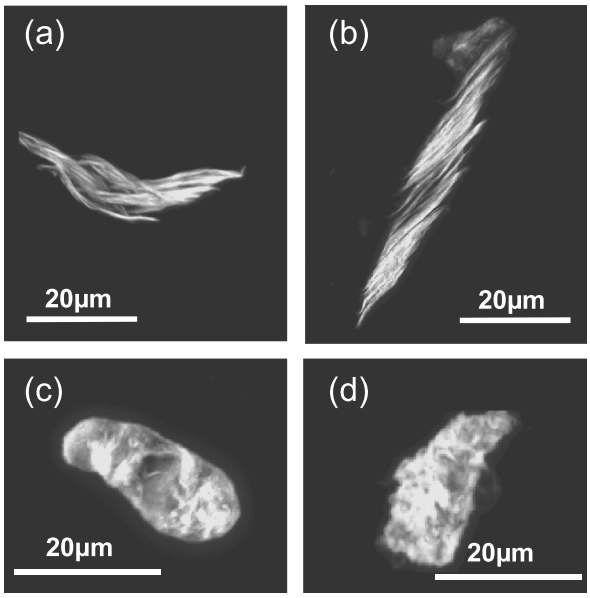

Fig. 7 Examples of the reconstructed morphology of actin filaments in the untreated FSMCs ((a) and (b)) and the contracted FSMCs ((c) and (d)).

cells were much stiffer in their major axis direction than in their minor axis; (b) such mechanical anisotropy disappeared under contraction; and (c) fleshly isolated cells displayed actin filaments running almost parallel to the major axis of the cell, while contracted cells had entangled and bulk-like filaments that exhibited no preferential direction.

Matsumoto et al.[9] first measured the tensile properties of freshly isolated rat aortic SMCs, and reported that the initial stiffness S_{ini} and the initial normalized stiffness E_{ini} was 0.062 ± 0.021 N/m and 12.6 ± 3.8 kPa ($n = 8$), respectively. These values are statistically similar to those obtained in the present study for the direction of the major axis: $S_{ini} = 0.070 \pm 0.016$ N/m and $E_{ini} = 14.8 \pm 4.3$ kPa ($n = 5$). The cells were held in different ways in the two studies. It was confirmed that the difference in cell-holding method does not affect the measured value significantly. The initial stiffness in untreated FSMCs was not significantly different between their major and minor axis directions, while in contracted cells, the value was higher in the minor than in the major direction in the present study. Cells stretched in the direction of their minor axis revealed that the initial cross-sectional area of untreated and contracted cells perpendicular to this direction was about 4.5 times and 2 times larger, respectively, than that perpendicular to the major axis direction. Thus, the tensile properties of cells whose diameters perpendicular to the stretch direction were quite different should be estimated by normalized stiffness. The initial normalized stiffness for the major axis direction was significantly larger than that for the minor direction (Fig. 5), indicating that untreated FSMCs have mechanical anisotropy. Such anisotropy may be due to their intracellular components. It has been suggested that actin filaments play an important role in the mechanical properties of cells[4), (6), (13)]. The elastic modulus of actin filament bundles (stress fibers) has been reported to be about 3 MPa[14], and is much higher than that of whole cells ($1 - 10$ kPa)[9), (13), (15), (16)]. These findings indicated that actin bundles may affect cell stiffness.

In this study, we observed the morphology of actin filaments in FSMCs using a confocal microscope. The thick actin filament bundles were observed running almost parallel to their major axis direction in untreated FSMCs (Fig. 7 (a) and (b)). When the cell was stretched along the major axis direction, the actin bundles of the cell may have been able to efficiently resist the tension applied to the cell. When stretched in the minor axis direction, the actin bundles may not participate in resisting the tension. Thus, the cells may be softer when the stretch direction is perpendicular to the fiber direction.

We also measured tensile properties of contracted FSMCs. In this study, about 20% of the cells responded to agonists, and the cell shortening ε_s was about 30%. Ives et al.[17] isolated SMCs from the rabbit thoracic aorta with enzymatic digestion and examined their contraction response to agonists. They reported that not all of the cells responded to agonists ($5 - 50$% cells responded), and that cell shortening was $10 - 15$%. Our results were quantitatively similar to theirs, although cell shortening was much higher in the present study. The large measure of cell shortening may indicate the cells were healthy and that damage caused by the enzyme was relatively small.

Agonist-induced contraction may affect cell stiffness. Steven et al.[18] reported that cultured air-way smooth muscle cells stiffened when they were exposed to contractile agonists, and that the stiffness of cells contracted with serotonin treatment (10^{-5} M) increased to about 1.5 times that of untreated cells. In this study, the initial normalized stiffness of contracted FSMCs were ~6 times and ~20 times higher than that of untreated cells in their ma-

jor and minor axis directions, respectively. The increase was much higher in the minor axis than in the major, and the difference between the two directions disappeared (Fig. 5). The three-dimensional morphology of actin filaments in contracted FSMCs showed an aggregated structure without a preferential direction (Fig. 7 (c) and (d)). In the smooth muscle contraction process, actin-activated myosin motor activity is promoted, and actin and myosin slide over each other[19]. Due to such actomyosin-based contraction, each actin bundle may become entangled, closely packed together, and stiffened in the cells. Actin bundles formed in such a way may have no preferential direction. Thus, FSMCs may not only increase their stiffness, but also reduce their mechanical anisotropy.

Initial normalized stiffness E_{ini} and cell shortening ε_s along the direction of the major axis show a significant positive correlation. A cell showing large shortening may have multiple contractile apparatus and actin-myosin binding sites, and becomes stiffer than cells showing small shortening. In contrast, the relationship between E_{ini} and ε_s along the direction of the minor axis was insignificant. The reason for this result is unclear.

In this study, we observed the morphology of actin filaments in untreated and contracted FSMCs, but only discussed them qualitatively and in a two-dimensional perspective. We need to analyze the morphology with quantitative parameters, such as actin filament orientation with respect to cell axis, their length, thickness, volume, etc. We focused our attention only on actin filaments, and not on other intracellular structures, such as the nucleus. Caille et al.[20] measured the mechanical properties of the nucleus isolated from endothelial cells using the uniaxial compression test. They reported that the elastic modulus of the endothelial nucleus was of the order of 5 kPa, which was significantly higher than that of the cytoplasm (about 0.5 kPa). If there were a strong mechanical interaction between the actin filaments and nucleus of a cell, the position of the nucleus may affect the mechanical anisotropy of the cells. We need to know the magnitude of the effect the position of the nucleus has on mechanical anisotropy in untreated and contracted FSMCs. In this paper we only discussed the elastic properties of the cells. Cells are, however, also viscoelastic[21),(22)]. We are now planning to measure the anisotropic viscoelastic properties of the cells. The actin filaments in untreated FSMCs ran almost parallel to the direction of their major axis. This indicates that the shear modulus of such cells may be much lower than that of a homogeneous body. It would be interesting to know how normal moduli relate to shear moduli. This knowledge may also be important in determining the shear modulus of the smooth muscle-rich layer in the lamellar unit of aortas, whose significance in blood-vessel wall micromechnanics has been argued recently[23),(24)].

Acknowledgements

This work was supported in part by Grant-in-Aid from the Ministry of Education, Culture, Sports, Science and Technology, Japan (T. Matsumoto, Nos. 15086209, and 16360052).

References

(1) Mulvany, M.J., Hansen, O.K. and Aalkjaer, C., Direct Evidence that the Greater Contractility of Resistance Vessels in Spontaneously Hypertensive Rats is Associated with a Narrowed Lumen, a Thickened Media, and an Increased Number of Smooth Muscle Cell Layers, Circ. Res., Vol.43 (1978), pp.854–864.

(2) Warshaw, D.M., Mulvany, M.J. and Halpern, W., Mechanical and Morphological Properties of Arterial Resistance Vessels in Young and Old Spontaneously Hypertensive Rats, Circ. Res., Vol.45 (1979), pp.250–259.

(3) Cox, R., Comparison of Arterial Wall Mechanics in Normotensive and Spontaneously Hypertensive Rats, Am. J. Physiol., Vol.237 (1979), pp.159–176.

(4) Franke, R.P., Grafe, M., Schmittler, H., Seiffge, D., Mittermayer, C. and Drenckhahn, D., Induction of Human Vascular Endothelial Stress Fibers by Fluid Shear Stress, Nature, Vol.307 (1984), pp.648–649.

(5) Sato, M., Nagayama, K., Kataoka, N., Sasaki, M. and Hane, K., Local Mechanical Properties Measured by Atomic Force Microscopy for Cultured Bovine Endothelial Cells Exposed to Shear Stress, J. Biomech., Vol.33 (2000), pp.127–135.

(6) Wang, H.C.J., Goldschmidt-Clermontb, P., Willea, J. and Yin, C.P.F., Specificity of Endothelial Cell Reorientation in Response to Cyclic Mechanical Stretching, J. Biomech., Vol.34 (2001), pp.1563–1572.

(7) Matsumoto, T., Yamamoto, M., Seo, S., Sato, J. and Sato, M., Effect of Hypertension on Contractile and Mechanical Properties of Smooth Muscle Cells Isolated from Rat Thoracic Aortas, Proc. 2001 Bioengng. Conf., (2001), pp.613–614.

(8) Matsumoto, T., Yamamoto, M., Nagano, Y. and Sato, M., Effect of Smooth Muscle Contraction on Their Mechanical Properties: Comparison with the Whole Wall Properties, Proc. 41st Conf. the Japan Society of Medical Electronics & Biological Engineering, (2002), p.132.

(9) Matsumoto, T., Sato, J., Yamamoto, M. and Sato, M., Smooth Muscle Cells Freshly Isolated from Rat Thoracic Aortas are Much Stiffer than Cultured Bovine Cell: Possible Effect of Phenotype, JSME Int. J., Ser. C, Vol.43, No.4 (2000), pp.867–874.

(10) Chamley, J., Campbell, G. and McConnell, J., Comparison of Vascular Smooth Muscle Cells from Adult Human, Monkey and Rabbit in Primary Culture and in Subculture, Cell Tissue Res., Vol.177 (1977), pp.503–522.

(11) Shue, G.H. and Brozovich, F.V., The Frequency Response of Smooth Muscle Stiffness during Ca^{2+}-Activated Contraction, Biophys. J., Vol.76 (1999), pp.2361–2369.

(12) Smith, P.G., Roy, C., Fisher, S., Huang, Q. and

Brozovich, F.V., Cellular Responses to Mechanical Stress: Selected Contribution: Mechanical Strain Increases Force Production and Calcium Sensitivity in Cultured Airway Smooth Muscle Cells, J. Appl. Physiol., Vol.89 (2000), pp.2092–2098.

(13) Nagayama, K., Nagano, Y., Sato, M. and Matsumoto, T., Effect of Actin Filament Distribution on Tensile Properties of Smooth Muscle Cells Obtained from Rat Thoracic Aortas, J. Biomech., (in press).

(14) Deguchi, S., Ohashi, T. and Sato, M., Single Stress Fibers Isolated from Vascular Smooth Muscle Cells Possess Surprisingly High Extensibility, Proc. ASME Summer Bioengng. Conf., (2003), p.833.

(15) Miyazaki, H., Hasegawa, Y. and Hayashi, K., Tensile Properties of Contractile and Synthetic Vascular Smooth Muscle Cells, JSME Int. J., Ser. C, Vol.45, No.4 (2002), pp.870–879.

(16) Wang, N., Mechanical Interactions among Cytoskeletal Filaments, Hypertension, Vol.32 (1998), pp.162–165.

(17) Ives, H.E., Schultz, G.S., Galardy, R.E. and Jamieson, J.D., Preparation of Functional Smooth Muscle Cells from the Rabbit Aorta, J. Exp. Med., Vol.148 (1978), pp.1400–1413.

(18) Steven, S.A., Rachel, E.L., Jean L., Rick, A.R. and Jeffrey J.F., Stiffness Changes in Cultures Airway Smooth Muscle Cells, Am. J. Physiol. Cell Physiol., Vol.283 (2002), pp.792–801.

(19) Somlyo, A.P. and Somlyo, A.V., Signal Transduction and Regulation in Smooth Muscle, Nature, Vol.372 (1994), pp.231–236.

(20) Caille, N., Thoumine, O., Tardy, Y. and Meister, J.J., Contribution of the Nucleus to the Mechanical Properties of Endothelial Cells, J. Biomech., Vol.35 (2002), pp.177–187.

(21) Sato, M., Theret, D.P., Wheeler, L.T., Oshima, N. and Nerem, R.M., Application of the Micropipette Technique to the Measurement of Cultured Porcine Aortic Endothelial Cell Viscoelastic Properties, J. Biomed. Engng., Vol.122 (1990), pp.263–268.

(22) Thoumine, O. and Ott, A., Time Scale Dependent Viscoelastic and Contractile Regimes in Fibroblasts Probed by Microplate Manipulation, J. Cell Sci., Vol.110 (1997), pp.2109–2116.

(23) Matsumoto, T., Goto, T., Furukawa, T. and Sato, M., Residual Stress and Strain in the Lamellar Unit of the Porcine Aorta: Experiment and Analysis, J. Biomech., Vol.37 (2004), pp.807–815.

(24) Matsumoto, T., Goto, T. and Sato, M., Microscopic Residual Stress Caused by the Mechanical Heterogeneity in the Lamellar Unit of the Porcine Thoracic Aortic Wall, JSME Int. J., Ser. A, Vol.47, No.3 (2004), pp.341–348.